

An Attempt to Calibrate the Laser Induced Fluorescence (LIF) Signal used for Oil Film Thickness (OFT) Measurements in Simulating Test Rigs

P.S. Dellis^a

^aSchool of Mechanical Engineering Educators, ASPETE Greece City of Athens Culture, Sports and Youth Organization, 50 Akadimias Str., 10679, Athens, Greece.

Keywords:

Piston-ring lubrication
LIF measurements
LIF calibration
Dynamic and static calibration methods
Simulating test rig

ABSTRACT

The issue of laser induced fluorescence calibration for engine and simulating rigs was studied using both a static calibration rig and a dynamic method involving a modified piston-ring specimen. The technique used to measure oil film thickness was laser induced fluorescence through optical fibres. Previous experimental studies have been conducted in test rigs and engines to obtain in-situ results showing the uncertainties lying within every applied method. In this study a comparison of two proposed methods is performed – bench calibration (micrometer based) and dynamic for a single piston-ring test rig application. Engine in-situ calibration was not an option so that uncertainties that follow the direct measurements in the piston cylinder engine assembly and the difficulty in determining the exact properties of the lubricant at the ring-pack, which simultaneously affect fluorescence (e.g. local temperature at point of measurement, lubricant degradation) could be avoided. A temperature parametric study of the dynamic calibration coefficient is also presented and a comparison between results from capacitance transducer minimum oil film thickness measurements and the LIF measurements. The discussion that follows the results, tries to enlighten the reasons behind inconsistencies found between the proposed methods.

Corresponding author:

Polychronis S. Dellis
School of Mechanical Engineering
Educators, ASPETE Greece
City of Athens Culture,
Sports and Youth Organization,
50 Akadimias Str., 10679,
Athens, Greece.
Email: pasd@city.ac.uk

© 2015 Published by Faculty of Engineering

1. INTRODUCTION

Currently, there is considerable interest in reducing the already low level of oil consumption in passenger car engines, through controlling the oil film thickness in between and under the piston-rings and the cylinder liner. Engine tribology is one of the major issues

affecting overall engine performance as well as a considerable amount of total energy losses. Numerous studies about elasto-hydrodynamic and hydrodynamic lubricant film thickness measurements eventually guided engine technology towards tribology reduction losses, via the formulation of new lubricants (additive technology, physical properties enhancement), a

more controlled oil transport through the ring pack and the formulation of the proper lubricant film in the piston-liner interface.

LIF experimental techniques comprising a LASER light source coupled with custom made fiber probes proved to be a promising method to study the variation of OFT in between and under the piston-rings. In an engine or a simulating test rig LIF experimental set-up, calibrating the film thickness directly from the voltage output of the photo multiplier is theoretically possible but requires an exact knowledge of how much laser light is transmitted to the oil film and the proportion of the resulting fluorescent light that reaches the cathode of the photomultiplier. Due to the difficulties of measuring these effects, it is necessary to develop some means of calibration instead [1].

The calibration of the LIF signal has been a major challenge. Smart and Ford [2] used light by a mercury lamp to illuminate the lubricant film on a spinning shaft. For the calibration of the signal, they used a known volume of oil over a known surface area. The calibration was found to be nearly linear with the exception of thicker lubricant films. Ting [3] suggested grooves on piston-ring for the calibration of the LIF signal. Hoult et al [4] made the first attempt to calibrate in-situ the measurement of oil film thickness in the piston-ring zone of a firing engine fitted with quartz glass window. Two independent methods were used: A bench calibration was performed using lubricant films of constant, known thickness. Dynamic calibration, which involves discerning a ring contour from the fluorescent intensity measured as a voltage versus time, during engine operation as the ring passes through the beam.

Calibration was performed with marks on piston by Lux et al [5]. For their experiments they used a fired single cylinder diesel engine with quartz window. They concluded that large differences were found between the statically and dynamically obtained calibration coefficients. The dynamically obtained coefficients varied with speed and load owing to the varying temperature.

Wong and Hoult [6] used two identical small production IDI diesel engines and five different ring configurations. For the calibration three

chemically etched marks of known depths were created on the piston, to provide distinguishing marks for calibration in addition to the scraper ring profile.

Richardson and Borman [7] suggested that the method of ring profile fitting has to deal with problems arising from oil starvation and ring twist. Small steps were used for calibration. Dynamic Calibration: Calibration steps were ground into the third piston-ring. Static calibration: The researchers proposed a bench top fluorescence calibration cell that continuously varied the film thickness.

Brown et al [8] proposed an in-situ calibration method with grooves in the piston skirt and top compression ring with depths that are readily machined or spark eroded (i.e. > 25 μm). The intensity of the fluorescing signal suggested that the grooves were continuously under-filled rendering them unsuitable for calibration purposes. A bench-top calibration procedure was chosen instead.

Phen et al [9] proposed ring profile fitting for calibration but it is subject to serious error due to variation of reflectance (and reflection characteristics of the ring and piston) over the ring surface. The static test rig showed that the calibration was linear.

Scanning LIF was applied to a transparent and a normal cylinder with quartz window from Konomi et al [10]. It is suggested that the absolute value of lubricant film thickness can be obtained from the data at a groove of known depth produced on a piston wall where oil is sufficiently applied.

Dearlove and Cheng [11] used a reciprocating test rig to measure friction of a single piston-ring against a liner segment. A chemically etched calibration groove on the ring, 25 μm deep and 150 μm long was used.

Measurements of minimum oil film thickness with the capacitance technique were presented by Stiyer and Ghandi [12]. At the minimum oil film thickness the capacitance technique provides an accurate measurement of the ring-wall distance and this value is used as a reference for the photomultiplier voltage, giving a calibration coefficient.

Froelund et al. [13] used a 4 cylinder spark ignition engine, LIF focusing probe at 83 % down from TDC. For the calibration procedure, toolmarks on the piston skirt found by surface roughness measurements are compared with the raw LIF signal from the same piston skirt region.

Nakayama et al. [14] proposed both a static and dynamic calibration method used for their measurements of oil film thickness in an engine bearing. The static calibration method is based on a test rig that has a known oil film thickness that is formed by two thickness gauges. On the other hand, the dynamic calibration is based on a step created by two gauges of known thickness.

Arcoumanis et al. [15] proposed a static calibration method for the Lister-Petter single cylinder diesel engine LIF results. The method consists of a micrometer of enhanced resolution and makes use of an optical fiber mounted flush with the anvil of a micrometer.

In Duszynski [16] a quantitative study is performed of the temperature effect on the calibration coefficients of all the engine oils tested in a Lister Petter diesel engine with a custom made calibration apparatus. It consists of 20 x 20 x 100 mm block of fused silica on which the calibration standard was in the form of grooves of known depth. For the thinnest oil film thicknesses, the lowest repeatability of the calibration procedure was observed. Therefore, obtaining calibration coefficients of high accuracy in the region between 0 and 10 μm is vital for improving the accuracy of the LIF system. Sampling the LIF signal while changing the temperature of the whole apparatus, enabled calibration coefficients for the engine oils at elevated temperatures to be obtained.

1.1 Fluorescence Theory - Temperature Effect

The phenomenon of fluorescence can be considered as a natural consequence of absorption of a quantum radiation of sufficient energy. Absorption of energy is a rapid process completed within one period of oscillation of the electronic field of the excitation source.

The combination of fiber optics and laser induced fluorescence for measuring the oil film thickness is a non-intrusive method.

Fluorescence arises when molecules in the oil film which are electronically excited due to photon absorption, subsequently relax to their ground electronic state within a few nanoseconds. Spectral discrimination of this emission can be readily achieved by appropriate optical filtering. The intensity of the fluorescence is related to the thickness of the oil film. Since this method is measuring actual oil volume, oil films on the cylinder wall can be examined throughout the cycle.

Environmental factors such as temperature can bring about significant changes in the viscosity of engine oils and their fluorescence spectra. In liquid oils, where the probability of collisional quenching is high, an increase of temperature will normally disturb the stability of molecules in the excited state and will have a marked effect on the characteristics of fluorescence emission.

As a consequence, increasing the temperature decreases fluorescence emission. This statement, however, is a very general one as there might exist circumstances in which the effect of temperature could be found to be quite the opposite.

The fluorescing properties of dyes can be permanently or temporarily affected by temperature. First of all, for any dye if the temperature is elevated high enough, the chemical structure of molecules will be modified and the dye will lose its ability to fluoresce. This phenomenon, which is called thermal bleaching, must be avoided by choosing dyes that can stand the temperature variations experienced by the dye/solvent solution. Secondly, below the thermal bleaching temperature, the absorptivity (ϵ_{dye}), and the quantum yield efficiency (ϕ) and the absorption and emission of a dye are function of temperature. Absorptivity usually decreases as temperature increases. According to Schäfer [17], the decay of absorptivity results from a broadening of the absorption spectra induced by an increased molecular vibration level. This is also related to the increased level of molecular vibration (Schäfer, [17]; Guilbault, [18]; Duarte and Hillman, [19]). In many solvents and certainly in engine oil, the viscosity dependency of the fluorescence efficiency will result in an additional temperature decay of fluorescence. Eventually, as long as the chemical structure of the dye molecule is not altered, the temperature effects are reversible [20].

1.2 Other tribological factors affecting the oil film

It is also essential to point out the effect of other tribological factors to oil film formation. The surface irregularities in conjunction with the type of lubricant play an important role to the engine performance and life. Zavos and Nikolakopoulos [21] examined their effect and it was found that the local maximum hydrodynamic pressures of worn surfaces promote the oil film distribution along the piston-ring thickness. Another group of researchers have stated that by optimizing the material of piston-rings largely, friction losses can be reduced. The reason for this is the high share of piston-rings (24 %) due to friction forces in the engine. Reducing friction in reciprocating machines can be achieved by using appropriate materials and optimizing the structure of the piston and piston group [22]. Surface roughness plays also a major role in the development of the science and technology of lubrication. Kumar and Rao [23] focused on the effect of surface roughness in squeeze film lubrication of two parallel plates. Load capacity and squeezing time increases with an increase in surface roughness asperities.

2. EXPERIMENTAL SET-UP

2.1 Single-ring simulating test rig

The experimental test rig used for the experiments is a simplified test rig representing a real internal combustion engine where a steady piston-ring section of overall width 5 mm is placed under a flat surface used as a reciprocating liner. The test rig was initially developed by Ostovar [24] and was later modified by Dellis [25]. The liner is made of heat treated gauge steel and secured (glued with high temp curing epoxy) in an aluminium block [25]. The simulation of the lubricant flow between the piston-ring and liner is accomplished by means of recirculation of the lubricant which is injected at the ring-liner interface via a temperature controlled tank. A K-type thermocouple is placed just before the holes of the oil collector, where the lubricant is injected at the ring-liner interface to control the temperature of the lubricant at the injection points. Oil injectors ensure that lubrication is fully flooded at all times during testing. A schematic of the

simplified test rig can be seen in Fig. 1a. Figure 1b shows a close-up of the oil injectors and the piston-ring specimen as it sits under the reciprocating liner.

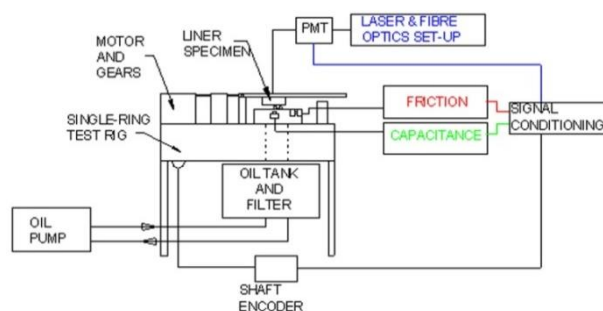


Fig. 1a. Single-ring test-rig schematic diagram.

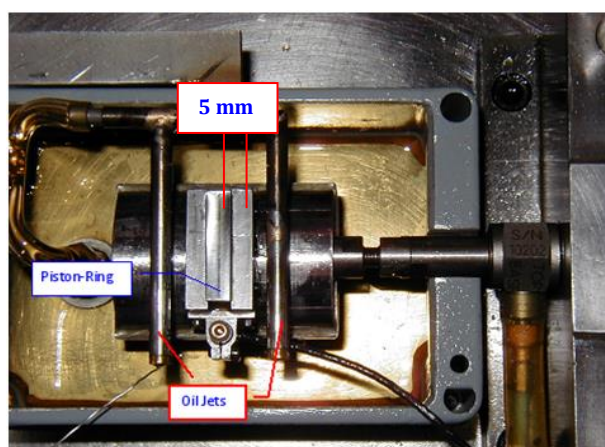


Fig. 1b. Close-up of piston-ring and oil injectors.

A variable speed DC electric motor coupled with nylon gears is used for the liner reciprocation. The motor is mechanically isolated from the rig to minimise any vibrations. The liner holder is connected to the drive mechanism by a removable connecting joint allowing access to the ring specimen. The ring specimen is fixed in the ring holder which is attached to the base. The ring holder sits on a knife edge which allows it to tilt in the transverse direction ensuring good conformity between the ring and the liner.

The piston specimen is made of high speed steel, shaped as rectangular paralleliped. Their curvature was ground on one side of it. The width of the piston-ring specimen is 5 mm, length 25.4 mm and height 8 mm with a radius of curvature 89.05 mm.

2.2 Data acquisition

The LIF signal was sampled 2000 times per revolution that allows a good spatial resolution

to be obtained. National Instruments SC-2345 signal conditioning unit with a National Instruments 16-bit 6035E PCI data acquisition card were used. The National Instruments NI-DAQ 6.9.3 was used for the development of the data acquisition program.

2.3 Laser apparatus and fiber optic set-up

An air-cooled argon-ion laser operating at a wavelength of 488 nm provided the excitation light. The laser power was adjusted to 50 mW. A wavelength selective beam splitter (dichroic mirror) reflecting blue laser light and transmitting green fluorescent light emitted by the measured lubricant film (514 nm) was used to direct the laser beam towards the fiber coupler. The low back reflection fiber coupler is capable of accommodating beams between 0.6 and 1.2 mm. The optical fiber was a graded index multimode fiber with a 30 μm - thick aluminium protective coating capable of withstanding temperatures of up to 400 $^{\circ}\text{C}$. The diameter of the core of the fiber is 50 μm , the cladding 125 μm and the outer diameter of the coating 175 μm . The fluorescent light was detected by the Hamamatsu 982 photomultiplier tube.

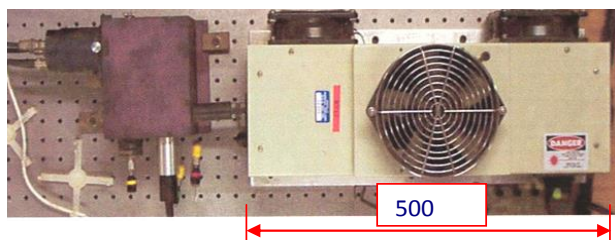


Fig. 2a. The Argon-Ion Laser with the fiber optics connection.

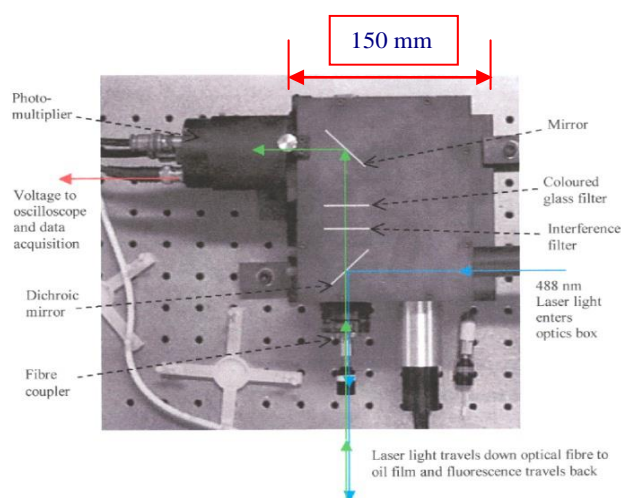


Fig. 2b. Fiber optics set-up with the fiber coupler, dichroic mirror and photomultiplier tube [15].

The filters comprised an orange glass filter with an edge wavelength of 530 nm and a band-pass interference filter.

2.4 LIF static calibration test rig

Duszynski [16] and Pyke [26] performed the static calibration with a high resolution micrometer. Thus, the thickness of the oil film flowing through the interrogation zone could be read from the scale of the micrometer. The oil for calibration is pumped from a small reservoir through the micrometer gap, with a pressure of 50 kPa. A typical response signal of the PMT (Photo Multiplier Tube) to a continuously changing oil film thickness in the calibration micrometer is shown in Fig. 3.

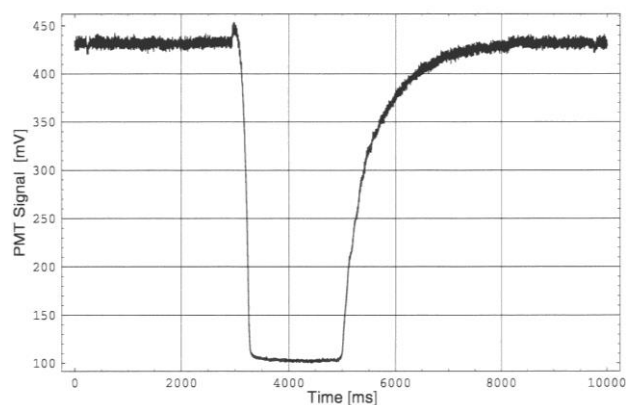


Fig. 3. Performance of the calibration micrometer-LIF signal [1].

Figure 3 shows the resulting LIF signal in mVolts first at a micrometer gap of 500 μm , then at its closure and reopening above the initial gap width. For the oil tested, widening the micrometer gap further did not cause any increase in the voltage signal. An obvious conclusion is that this LIF system cannot be used for oil film measurements thicker than 500 μm . The limited range, however, has no effect because according to Duszynski (1999) [16] engine experiments, the lubricant film thickness between the piston rings and the cylinder liner was found to be within the range 0-10 μm .

The static calibration method (Figs. 4a, 4b and 4c) showed very low repeatability for the data points corresponding to an oil film thickness of 10 μm . Even for zero film thickness the photomultiplier would normally detect a signal of very low level. This offset is present in the LIF signal throughout the experimental work.

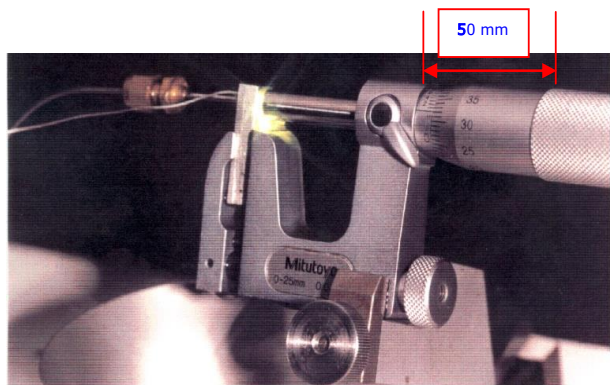


Fig. 4a. Layout of the static calibration micrometer based test rig.

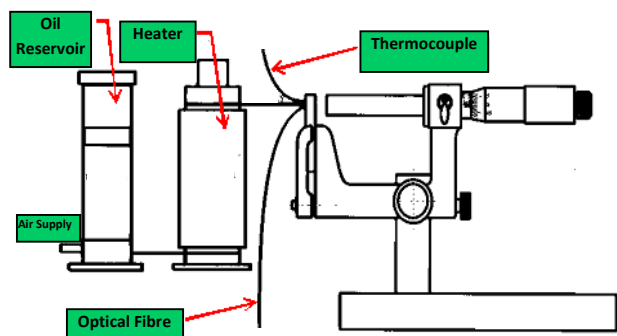


Fig. 4b. Schematic of the technique.

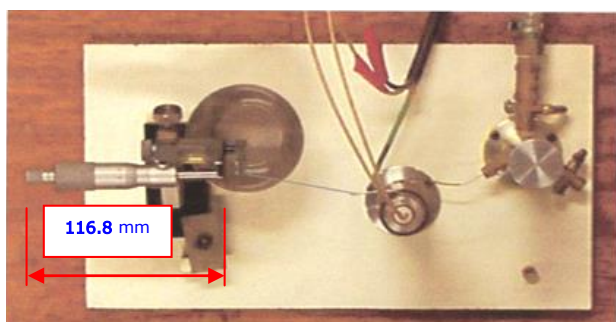


Fig. 4c. Photo of the static calibration test rig [16].

2.5 LIF Dynamic Calibration – Piston-ring specimen

For the purpose of LIF dynamic calibration, a piston-ring specimen was modified to be used for the experimental set-up of the single ring test rig according to the specifications in Fig. 5. The dynamic calibration is based on etching a groove or grooves of known depth on the surface where the optical fiber travels above.

Figure 6 shows a photo of the ring specimen with the Electrical Discharge Machining (EDM) - machined groove attached to the ring holder.

The requirements for machining the groove are:

- Surface finish of the groove: the best possible the spark eroding machine (EDM) can provide (ideally Roughness average, (R_a) $< 1 \mu\text{m}$).
- Depth of the groove: It should be between 15 and 25 μm .

The first attempts were not satisfactory due to the “rough” finishing of the spark eroded surface. A sample of the “rough” finish of the unsatisfactory groove can be seen in Fig. 7.

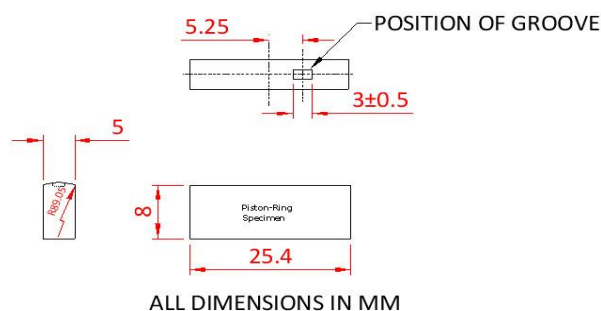


Fig. 5. Drawing of the piston ring specimen used for dynamic calibration.

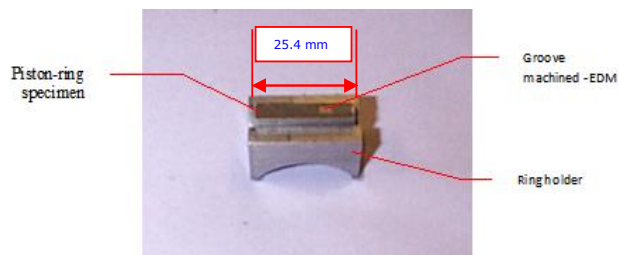


Fig. 6. The groove on the surface of the piston-ring fixed in the ring holder (length and width of piston-ring specimen can be seen in Fig. 5).

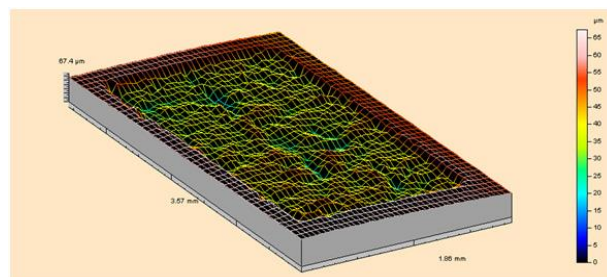


Fig. 7. First unsuccessful attempt to etch groove on the surface of the piston-ring with EDM (groove depth varies from 0 to 65 μm).

According to Fig. 7, the groove depth varies from 0 μm to 65 μm .

A specially made piston ring specimen the material of which is most suited for spark erosion machining was manufactured. A Cu-Cr-

Zr (copper-chromium-zirconium) spark erosion electrode was used, and to enhance the accuracy of the manufacturing procedure, the spark erosion technique was applied for a significantly longer period of time than in the past “failed” attempts. The surface profile of the new piston-ring specimen was measured in the Talysurf surface profilometry and a satisfactory surface finish was achieved (Figure 8). A radius of 89.0513 mm for the upper curved surface was measured. Figure 9a and Figure 9b show the quality and the depth of the groove.

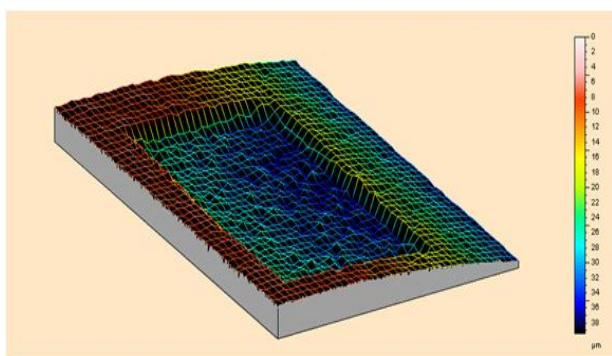


Fig. 8. Three dimensional meshed axonometric of groove.

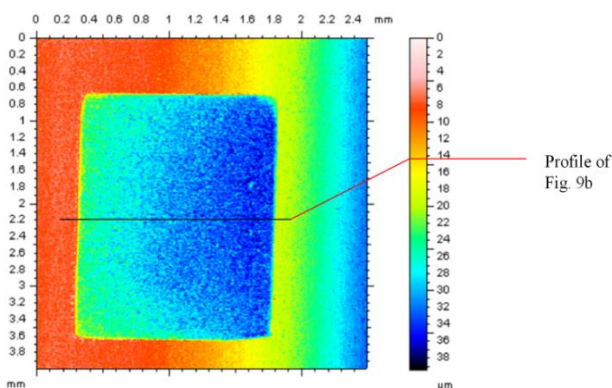


Fig. 9a. Two dimensional coloured surface roughness of the groove. (Fig. 9a).

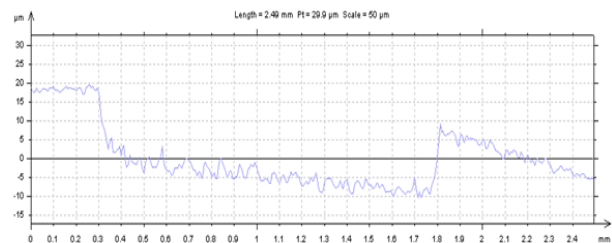
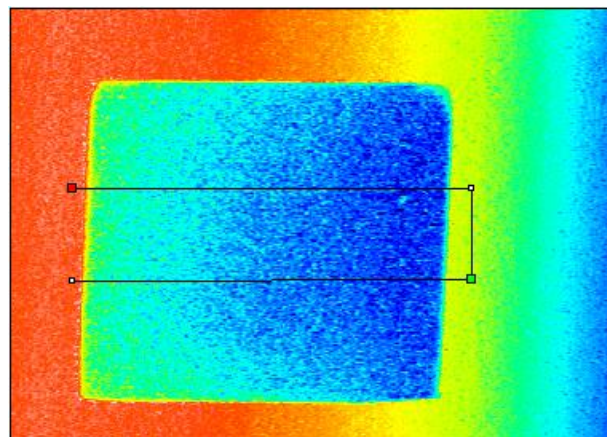


Fig. 9b. Marked groove profile from Fig. 9a (Fig. 9b).

Figure 10 shows that the groove dimensions set according to the requirements were met with the best possible results.



	Hole	Peak
Surface (mm ²)	1.35	0.0777
Volume (mm ³)	0.0211	8.9e-005
Max. depth/height (µm)	23.3	6.66
Mean depth/height (µm)	15.7	1.14

Fig. 10. Maximum and mean depth of the marked volume on the groove surface.

2.6 Lubricant properties of tested oils

For the parametric study, CASTROL lubricant coded 003B was used with the following properties (Table 1).

Table 1. Tested lubricant properties.

CASTROL Code	003B
SAE Grade	0W-30
Viscosity Index	182
V ₁₀₀ (cSt)	12.16
V ₄₀ (cSt)	68.93
HTHS (mPa s)	3.30
Polymer	Castrol Code A
Base Fluid	Poly alpha olefin

V₁₀₀: Kinematic Viscosity at 100 °C

V₄₀: Kinematic Viscosity at 100 °C

HTHS: High Temp High Shear viscosity

3. RESULTS

3.1 LIF Results - Static Calibration Test Rig

A series of tests were carried out to compare the static calibration coefficient with the ones derived from dynamic calibration that will follow further on (see LIF results – dynamic calibration). Static calibration tests were carried out with the micrometer based test rig following the method described at Duszynski [16].

The results were taken at an average oil temperature of 40 °C. The test conditions for oil 003B were set at 50 mW laser power, 0.39 kV (voltage at PMT tube). The points and trendline are calculated from 10 microns and onwards, as data below 10 microns have no trend and therefore are not included in the calculations (Fig. 11).

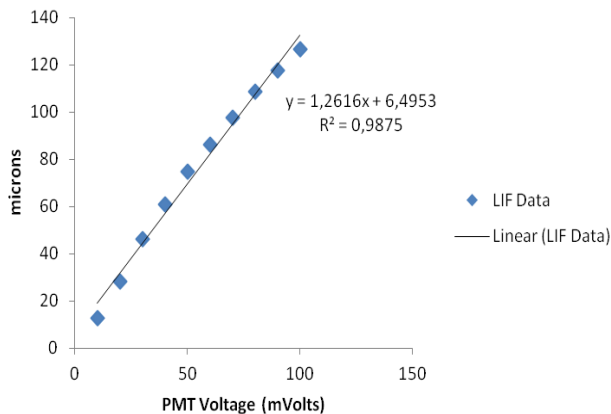


Fig. 11. Static LIF calibration for Oil 003B, 0.39 kV, 50 mW laser power.

The calibration coefficient derived is 1262 $\mu\text{m}/\text{Volts}$ (according to Fig. 11).

3.2 LIF Results - Dynamic Calibration

The dynamic LIF calibration coefficient was derived when the groove data versus the LIF data acquired were matched.

Groove data were acquired at the area where the fitted fiber on the liner specimen travels. Since the stylus of the profilometer was acquiring data for the groove every 10 μm of groove length, five (5) profiles in sequence have been averaged (all profiles are similar to Fig. 12) to get the data that were going to be compared to the LIF signal (the diameter of the fiber core is 50 μm). Eventually the area of the groove over which the fiber travels was covered in the best way possible.

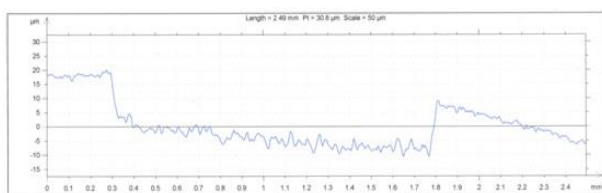


Fig. 12. A Groove profile starting every 10 μm from the edge of the fiber diameter: profile at 10 μm .

The groove data of the five (5) profiles (profiles are similar to Fig. 12) were averaged so that a mean value of the groove profile could be derived (see Fig. 13). This value is going to be used for the LIF dynamic calibration experiments. The datum at the averaged groove profile is the reference point used for superimposing groove data versus LIF data.

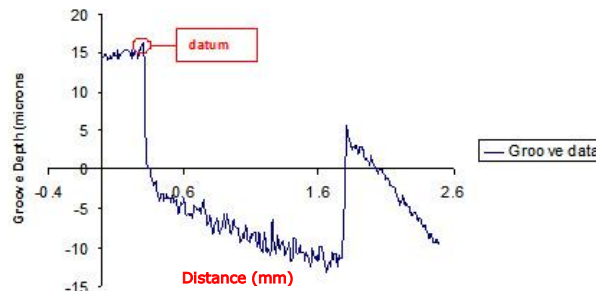


Fig. 13. The averaged profile for the piston-ring specimen over which each LIF signal is going to be calibrated.

Figure 14 shows a schematic of the groove area over which the optical fiber travels.

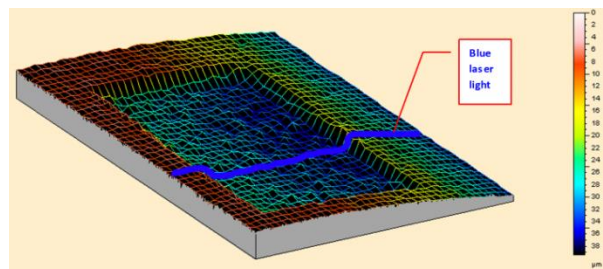


Fig. 14. The groove with the blue - highlighted line shows the area over which the optical fiber travels.

3.3 LIF Dynamic Calibration Experimental Set-up - Results

The stroke was set at 5 mm, which is close to the shortest stroke value that can be achieved in the single-ring test rig when adjusting the liner's connecting threads. This way the amount of data acquired per stroke is ensured to be as many as possible by the data acquisition system when the fiber travels on top of the piston groove, the width of which is 1.525 mm, thus ensuring highest number of LIF data to be acquired over the groove, and consequently improving the accuracy of the technique. Then, data were acquired with a 37-40 °C oil temperature, at different speeds and loads. Every experiment was run for 20 cycles and each cycle from the LIF data was checked individually so that the

ones that were bubble free to be chosen for the calibration procedure. Then, the LIF data were averaged and a mean LIF curve from the filtered data was taken. The LIF curve and the groove data were placed on top of each other and a calibration coefficient was derived graphically using a MATLAB program as seen in Fig. 15. The matching was repeated for every experimental condition that was chosen from the beginning of the tests and in the end the calibration coefficient was taken as the statistical average of each individual matching measurement. The appearance of bubbles in the groove is a major source for uncertainties, because they interfere with the LIF signal, as the groove is not entirely filled with lubricant. The appearance of bubbles interferes with the LIF signal giving erroneous results when the calibration coefficient is derived. During this process, such erroneous results were omitted.

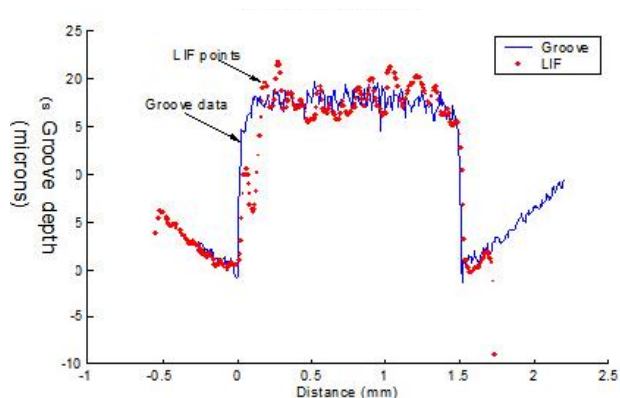


Fig. 15. Matching of groove data and averaged LIF data.

For oil 003B the calibration coefficient is $295 \frac{\text{microns}}{\text{Volts}}$ at 38°C, 0.39 kV PMT voltage, 50 mW laser power. This coefficient is the mean average of each one of the best fitted LIF signals (24 signals in total) against the groove data (bubble free signals).

3.4 Minimum Oil Film Thickness Comparison between Capacitance and LIF Measurements

An attempt to get a clear picture of the reliability of the calibrated LIF results was achieved through a comparison between LIF and OFT capacitance results. Capacitance results from the simulating test rig are described in [27]. For the OFT capacitance results the same aluminium liner (same weight), oil (CASTROL 003B – Table

1) for various loads and 400 rpm speed was used [25] and they were directly compared to a respective experiment at the same testing conditions with the same liner at a different time. The repeatability of the capacitance and LIF results was documented before the extensive OFT, friction, temperature variation, pressure measurements and visualisation results were obtained [27,28]. The initial comparison showed that there is a big difference between the OFT measurements acquired with the capacitance probe and the LIF technique. No additional chromophore was used for the LIF results. The calibrated LIF results with the dynamic calibration method had a thickness under the piston-ring almost triple that of the capacitance results as shown in Figs. 16a, 16b and 16c.

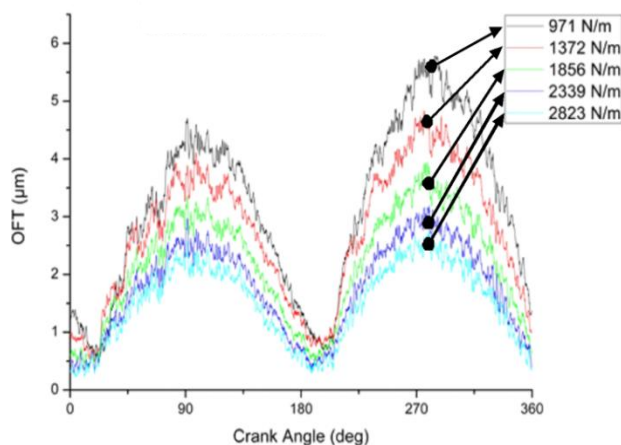


Fig. 16a. Load variation on capacitance OFT results for oil 003B at 400 rpm and 45 mm stroke [27].

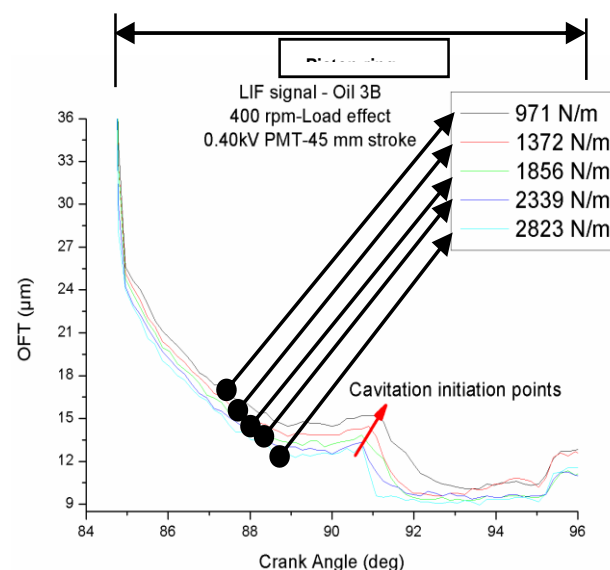


Fig. 16b. Load variation on LIF data (dynamic calibration) – downstroke.

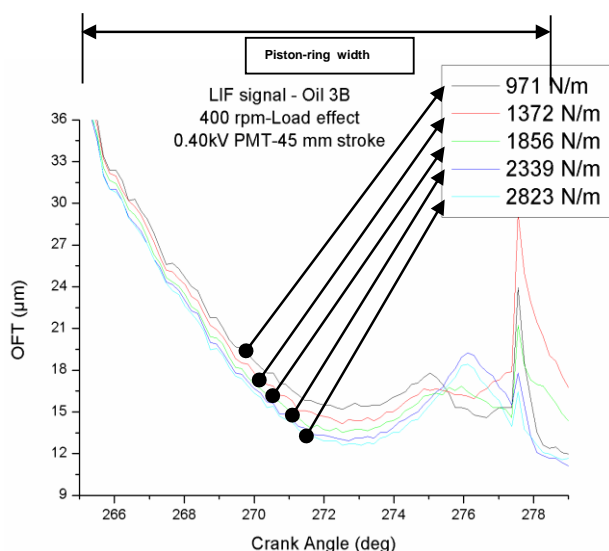


Fig. 16c. Load variation on LIF results (dynamic calibration) – upstroke.

The load variation on the capacitance and LIF signal is verified as seen in Figs. 16a, 16b and 16c, where the lower the load the thicker the oil film. The LIF results, calibrated with the dynamic calibration coefficient derived from the previous experiments at 38 °C, 0.39 kV PMT voltage, 50 mW laser power, have big discrepancies compared to the capacitance results.

3.5 Comparison between LIF Static and Dynamic Calibration

The calibration coefficient derived from the static calibration tests (1262 $\mu\text{m}/\text{Volts}$ at 40 °C) for the same oil at the same testing conditions as the dynamic method (295 $\mu\text{m}/\text{Volts}$ at 38 °C) provide less than encouraging results. Reasons behind this are the different laser power output from the optical fibers (the one on the liner surface and the one on the micrometer based test rig). The marginal temperature variations do not provide a good reason for this inconsistency as the difference in dynamic calibration coefficients from 38 °C to 40 °C lies within the test variations (derived from linear regression, Table 2). 38 °C oil temperatures at the simulating test rig is ambient oil temperature plus the temperature from friction between the reciprocating surfaces, without using the oil heater.

Since different fibers are used for the experiments at the static calibration test rig, the use of this technique should be accompanied by

the fibers' laser power output measurements. A Spectra Physics 404 Power Meter was used to measure the aluminium liner fiber power output as it exits the surface of the liner used for the dynamic calibration experiments. This measurement is going to be compared to the power output of the fiber at the jig of the micrometer based test rig (static calibration method as described in previous section). The tests were carried out at 50 mW laser power and it was found that the two fibers were giving out power measurements that differ by 125 %; at 30 mW laser power the difference between the two power outputs was 20 %. So, any direct comparison between the two calibration methods, should take into account that the power output differs between various fiber optics fittings.

Table 2. Temperature results for the calibration coefficients.

Oil Temperature (°C)	38	50	60	70
Calibration Coefficient ($\mu\text{m}/\text{Volt}$)	295	364	353	389
St. Dev. ($\mu\text{m}/\text{Volts}$)	14	26.9	21	55.37
Error (%)	5	7	6	14

Furthermore, the laser power output was being reduced during the experiments, due to laser tube overheating. There is a substantial difference between static and dynamic calibration methods.

The reasons behind this are:

- a) Great difference between laser power outputs as different fibre installations are being used. To overcome this, for the measured laser power, a correction factor has to be introduced in the calibration measurements which are also stated by Richardson and Borman [7]. Lux et al [5] also concluded that the substantial difference between the in-situ calibration (piston tool marks) and bench method is due to reduced laser power and a 40 % uncertainty of the LIF film thickness measurement was also recorded by Dearlove and Cheng [11].
- b) Reduced laser power while testing for long periods of time, due to tube overheating of the air-cooled Argon-Ion Laser
- c) Bleaching effect of fluorescence is altered due to the above.

- d) Calibrating the LIF signal in the range of 0-5 μm for which the photobleaching effects might have a more pronounced effect on the fluorescence quantum yield of oil film thickness, might also compensate for some non-linear effects in the fluorescence signal which can be observed for very thin lubricant films [16].

Furthermore it should be taken in account that:

- LIF signal for the dynamic calibration method is affected by bubbles inside the groove. Bubbles are evident at high as well as at low temperatures. Their appearance is reinforced with increasing reciprocation speed and temperature. It is therefore essential to perform the dynamic calibration experiments at low speeds, using the single ring test rig.
- Bench calibration is not able to provide robust results at high temperatures due to thermal expansion of the micrometer and uncontrolled temperature level (Also pointed out by Duszynski [16]).

3.6 LIF Dynamic Calibration Variation with Temperature

In this paragraph the effect of temperature on the dynamic calibration coefficient is studied. For this experiment, similar set-up to previous paragraph (LIF dynamic calibration experimental set-up) was used and 4 different temperatures were chosen, 38, 50, 60 and 70 °C for the same lubricant. For every experimental set, 24 different experimental conditions were chosen as in the case of the previous paragraph (LIF dynamic calibration experimental set up – results), varying the speed and load each time so that data from different conditions (and as far as possible bubble free) can be acquired and compared before a mean value is derived.

Figure 17 represents the observed trend-the coefficient increases respectively with temperature. The dynamic coefficient results at high temperature have greater standard deviation of mean because of the accumulated bubbles in the calibration groove. Bubbles were noticed most of the time at higher temperatures and for calibration purposes they were omitted.

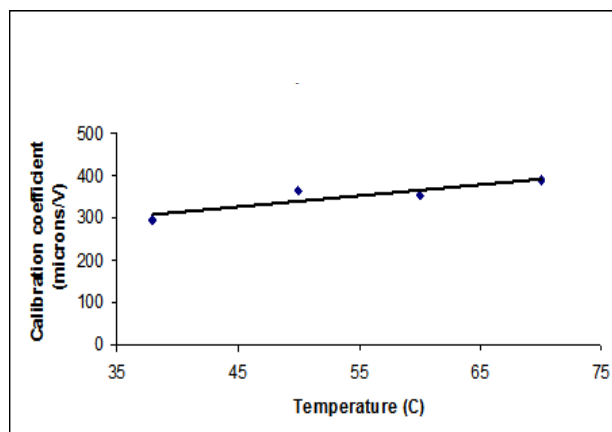


Fig. 17. Variation of the dynamic calibration coefficient with temperature (effect of temperature on fluorescence emission).

3.7 Background Noise Considerations

When the PMT is switched on, a shift on the PMT voltage is noticed. The PMT tube detects radiation which is derived from background ambient radioactivity. Such sources can be traces of long lived gamma-emitters in the bricks of the building or the concrete floor, ^{40}K in the glass of the photomultiplier and the sample vials, cosmic rays, traces of uranium in lead shielding, etc. There are also spurious counts which are not radioactive background and for which shielding does no good. They arise from PMT noise. Typical noise rates can be between 200 and 1000 pulses per second.

There are still other volume related sources of spurious counts. Though there is an extremely high vacuum within the PMT, there still remain many gas molecules. These occasionally interact with the electron avalanche in the region of the anode and become ionized. The ions migrate to the cathode where they are discharged, sometimes producing light. In general, the smaller tubes are to be favored over the larger ones. The advantage is not only in the lower mass, but also in their lower operating voltage which makes for less noise and less residual gas ionisation [25].

Repeated tests using the reciprocating test rig at slow speed without any lubricant present between the two surfaces, showed that the noise level that the PMT detects, has a mean value of 27.5 mVolts. Figure 18 shows this trend.

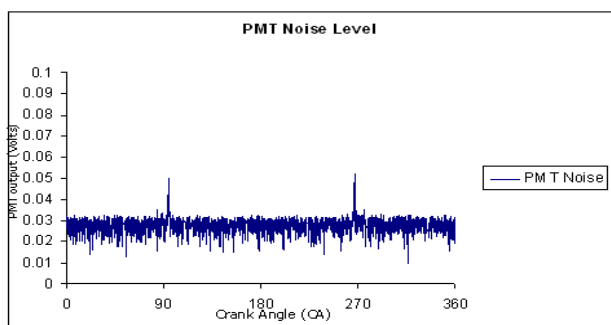


Fig. 18. PMT noise-background radiation level.

The peaks recorded at 90° and 270° are reflections of the piston ring specimen. This mean value has to be subtracted from the final LIF signal that will be calibrated. According to the dynamic calibration coefficient found for oil 003B at ambient conditions, this noise level that needs to be subtracted represents a total thickness value added on the film of 8 microns.

This offset was present in the LIF signal throughout the experiments and should be regarded as a typical characteristic of a fiber optic sensor. The following factors contribute to this inherent behaviour amongst which are the following:

- Dark current of the photomultiplier caused primarily by ohmic leakage
- Background signal such as reflections and background fluorescence of the optical fiber
- Fluorescence of the dichroic mirror (depends on the wavelength) [16].

3.8 Effect of Brightness

Figure 19 show how the different emitted laser light affects the LIF signal. If the brightness is very low, a different PMT voltage has to be applied in order to compensate for the loss of the signal.

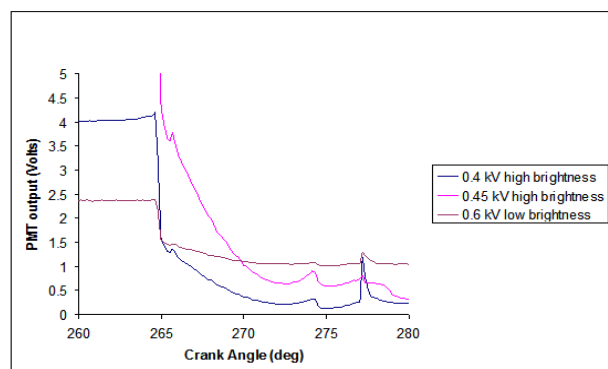


Fig. 19. Effect of brightness on LIF signal: differences in the emitted laser light affects the LIF signal.

4. SUMMARY/CONCLUSIONS

Dynamic calibration is needed in the oil film analysis because the LIF technique, when used for measurements, can provide repeatable results of the oil film thickness. It can be used as a mean of validating results that are derived from other methods, such as the capacitance technique. Findings in this research topic include:

- More focus on the small scale and trial to match the LIF signal with the surface roughness data was a key point in this research.
- When temperature rises, a higher mean calibration coefficient is derived verifying the trends already found in literature. Using these coefficients, though, requires knowledge behind the big error sources so that they will be omitted.
- PMT background noise is playing a major part as it is present throughout testing and it also affects the linearity of the calibration curve.
- If the measurement is less than 5 μm , which is the case for the minimum oil film thickness according to the capacitance results, it is not accurate because the ratio between the voltage and the thickness is too small. Obtaining calibration coefficients of high accuracy in the region of 0 to 10 μm is vital for improving the accuracy of the LIF system.
- In order to close the gap between static and dynamic LIF calibration coefficients, the simulating test rig will be fitted with a new temperature control, more direct and precise than the previous used for the experiments in this research. Eventually, the temperature setting could be as close as possible to the oil temperature at the point of LIF measurements.
- Problems related to full flooding of the groove have to be overcome. Even so, it has to be certain that the lubricant is bubble free. Bubbles in the calibration groove affect any direct conclusion about the dynamic calibration coefficient. So, in-situ measurements and direct calibration seem to have an inherent deficit that affects the random calibration of the LIF signal.
- It was essential for the development of the dynamic calibration technique: 1) to acquire

as many data as possible from the fiber optic sensor when it “travels” over the groove and 2) to achieve via EDM the smoothest possible groove surface.

- The implementation of such measurements in an engine application and to calibrate the LIF signal from fiber optic stations fitted to the length of the stroke and the circumference of the bore, simultaneous measurements of temperature at the point where the lubricant fluoresces have to be conducted, samples of the lubricant have to be studied for degradation and alteration of its fluorescing properties and a correction factor has to be added to compensate for laser power loss due to the fiber optics fittings and PMT noise-background radiation effect.

4.1 Novelties/Future Work

In this research topic the novelties can be summarized as follows:

- More focus on a smaller scale and trial to match the LIF signal with the surface roughness data was a key point in this research.
- Effect of bubbles in the calibration groove was pointed out even at low test rig reciprocation speeds and having already a fully-flooded calibration groove. Their appearance gives erroneous results when a calibration coefficient is derived. At higher temperature bubbles are more pronounced inside the calibration groove.
- The background noise in the PMT tube and the brightness of the emitted blue light from the fiber were also considered as affecting factors and tried to be quantified.
- The idea of using the single rig to eliminate uncertainties that are combined to engine operation such as ring twist, oil degradation and cavitation seemed to be convenient in order to acquire robust results that are much easier to interpret. The comparison, however, between static and dynamic LIF calibration gave less than encouraging results to proceed with such a comparison. Future work should include:
- Standard fiber fittings in the different test rigs so that variations of brightness/power

output remain within certain limits that do not affect the measurements.

- Use of a detailed oil temperature control for the simulating test rig
- Actions that lessen the background noise effect on the PMT tube signal.

Acknowledgments

The author would like to acknowledge the Greek State Scholarship Foundation for the support provided. The work has been conducted at City University, School of Engineering and Mathematical Science, Laboratory for Energy and the Environment under the supervision of Prof. C. Arcoumanis. The author also acknowledges the important contribution of Dr Y. Yan to the project during her time as a Senior Experimental Officer at City University London and Mr Kostas Lymeris, Mechanical Engineer Educator from ASPETE, Greece, for his persistence to proceed with this publication. The author also thanks CASTROL for providing the lubricants for the experiments.

REFERENCES

- [1] C. Arcoumanis, M. Duszynski, H. Lindenkamp and H. Preston, 'Measurements of oil film thickness in the cylinder of a firing diesel engine using LIF', *SAE 982435*, 1998.
- [2] A.E. Smart and R.A.J. Ford, 'Measurement of thin liquid films by a fluorescence technique', *Wear*, vol. 29, pp. 41-47, 1974.
- [3] L.L. Ting, 'Development of a Laser Fluorescence Technique For Measuring Piston Ring Oil Film Thickness', *Transactions of the ASME, Journal of Lubrication Technology*, vol. 102, pp. 165-171, 1980.
- [4] D.P. Hoults, J.P. Lux, V.W. Wong and S.A. Billian, 'Calibration of Laser Fluorescence Measurements of Lubricant Film Thickness in Engines', *International Fuels and Lubricants Meeting and Exposition*, Portland, Oregon, October 10-13, 1988.
- [5] J.P. Lux, D.P. Hoults and M.J. Olechowski, 'Lubricant Film Thickness Measurements in a Diesel Engine Piston Ring Zone', *Lubrication Engineering*, vol. 47, no. 5, pp. 353-364, 1991.
- [6] V.W. Wong and D.P. Hoults, 'Experimental survey of lubricant-film characteristics and oil

- consumption in a small diesel engine', *SAE Paper 910741*, 1991.
- [7] D.E. Richardson and G.L. Borman, 'Using Fiber Optics and Laser Fluorescence for Measuring Thin Oil Films with Applications to Engines', *SAE Paper 912388*, 1988.
- [8] M.A. Brown, H. McCann and D.M. Thompson, 'Characterisation of the Oil Film Behaviour Between the Liner and Piston of a Heavy-Duty Diesel Engine', *SAE Paper 932784*, 1993.
- [9] R.V. Phen, D. Richardson and G. Borman, 'Measurements of Cylinder Liner Oil Film Thickness in a Motored Diesel Engine', *SAE Paper 932789*, 1993.
- [10] T. Konomi, M. Murakami and S. Sanda, 'Effects of piston skirt profile on friction loss and oil film behavior', in *Experimental and Predictive Methods in Engine Research and Development*, 17-18th November 1993, National Exhibition Centre, Birmingham, pp. 147-154, 1993.
- [11] J. Dearlove and W.K. Cheng, 'Simultaneous Piston Ring Friction and Oil Film Thickness Measurements in a Reciprocating Test Rig', *SAE Paper 952470*, 1995.
- [12] M.J. Stiyer and J.B. Ghandhi, 'Direct Calibration of LIF Measurements of the Oil Film Thickness Using the Capacitance Technique', *SAE Paper 972859*, 1997.
- [13] K. Froelund, J. Schramm, B. Noordzij, T. Tian and V. Wong, 'An Investigation of the Cylinder Wall Oil Film Development During Warm-Up of an SI-Engine Using Laser Induced Fluorescence', *SAE Paper 971699*, 1997.
- [14] K. Nakayama, I. Morio, T. Katagiri and Y. Okamoto, 'A Study for Measurement of Oil Film Thickness on Engine Bearing by using Laser Induced Fluorescence (LIF) Method', Central R&D, Daido Metal Co., Ltd, *SAE 2003-01-0243*, 2003.
- [15] C. Arcoumanis, M. Duszynski, E. Pyke and H. Preston, 'Cold Start Measurements of the Lubricant Film Thickness in the Cylinder of a Firing Engine', *SAE Paper 982436*, 1998.
- [16] M. Duszynski, 'Measurement of Lubricant Film Thickness in Reciprocating Engines', *PhD thesis*, Imperial College of Science, Technology and Medicine, 1999.
- [17] F.P. Schäfer, *Topics in applied Physics Volume I, Dye Lasers*. New-York/Heidelberg/Berlin: Springer-Verlag, 1973.
- [18] G.G. Gilbault, *Practical Fluorescence: Theory, Methods and Technique*. New York: Marcel Decker, 1973.
- [19] F.J. Duarte, L.W. Hillman, *Dye Laser Principles with applications*. Quantum Electronics-Principles and Applications: Academic Press, 1990.
- [20] B. Thirouard, 'Characterization and Modeling of the Fundamental Aspects of Oil Transport in the Piston Ring Pack of Internal Combustion Engines' *PhD Thesis*, MIT, Department of Mechanical Engineering, June 2001.
- [21] A. Zavos, P. Nikolakopoulos, 'Effects of Surface Irregularities on Piston Ring-Cylinder Tribo Pair of a Two Stroke Motor Engine in Hydrodynamic Lubrication', *Tribology in Industry*, vol. 37, no. 1, pp. 1-12, 2015.
- [22] S. Milojević, R. Pešić, D. Taranović, 'Tribological Principles of Constructing the Reciprocating Machines', *Tribology in Industry*, vol. 37, no. 1, pp. 13-19, 2015.
- [23] J.V. Kumar, R.R. Rao, 'Effects of Surface Roughness in Squeeze Film Lubrication of Two Parallel Plates', *Tribology in Industry*, vol. 37, no. 2, pp. 161-169, 2015.
- [24] P. Ostovar, '*Fluid aspects of piston ring lubrication*', *PhD Thesis*, Mechanical Engineering Department, Imperial College of Science, Technology and Medicine, 1996.
- [25] P. Dellis, 'Aspects of lubrication in piston cylinder assemblies', *PhD Thesis*, Mechanical Engineering Department, Imperial College London, University of London, April 2005.
- [26] E.A. Pyke, 'Investigation of Piston Ring Lubrication Using Laser Induced Fluorescence', *PhD thesis*, Imperial College of Science, Technology and Medicine March 2000.
- [27] P. Dellis, 'Effect of friction force between piston rings and liner: a parametric study of speed, load, temperature, piston-ring curvature, and high-temperature, high-shear viscosity', *Proc. IMechE, Part J: J. Engineering Tribology*, vol. 224, no. 5, pp. 411-426, 2010.
- [28] P. Dellis and C. Arcoumanis, 'Cavitation development in the lubricant film of a reciprocating piston-ring assembly' *Proc. IMechE, Part J: J. Engineering Tribology*, vol. 2018, no. 3, pp. 157-171, 2004.